Water-Energy Nexus Perspectives in the Context of Photovoltaic-Powered Decentralized Water Treatment **Systems: A Tanzanian Case Study**

Bryce S. Richards, [a, b] Junjie Shen, [c, d] and Andrea I. Schäfer*[d, e]

Water and energy are inextricably linked in today's society. This paper broadly introduces the water-energy nexus before focusing on sub-Saharan Africa, where residents have the poorest access to both clean drinking water and electricity worldwide. Given that many of the affected people live in remote areas, new solutions are required to improve the quality of life. The potential of decentralized photovoltaicpowered membrane filtration systems for the provision of potable water is highlighted. In particular, the potential of

this technology is investigated for the removal of dissolved trace contaminants such as fluoride, which naturally occurs at extremely high concentrations in the water sources of northern Tanzania. Results from field research demonstrate the importance of matching the best membrane to a particular water source to achieve the highest permeate production that complies with drinking-water guidelines at the lowest specific energy consumption.

Introduction

The aim of this paper is threefold: First, it introduces the reader to the concept of water-energy nexus and the increasing importance that this plays in today's society. Second, the focus moves to sub-Saharan Africa (SSA), which is a special case due to the vast lack of infrastructure for the provision of water and electricity, especially in remote areas. The theory of the energy consumption of desalination processes is presented, particularly as a function of the salinity of the water, which is relevant in this paper due to the focus on treating brackish water by using solar power. Finally, a case study resulting from field work in Tanzania demonstrates the potential of small-scale photovoltaic-powered distributed systems for the provision of clean drinking water in remote locations, with a focus on the removal of fluoride, which is a major contaminant in the area.

Water-energy nexus

The water-energy nexus is a concept that relates the water used for energy production and, conversely, the energy consumed to supply and treat water. Thus, water and energy are inextricably intertwined. The extent to which the link between water and energy directly impacts today's society is illustrated in Figure 1.

Every kWh of electricity generated by any power plant has consumed some water during either manufacturing or operation. For instance, in large-scale hydropower systems, an average of 17 m³ of water is used to generate each MWh of electricity from the turbine.[1] For utility-scale electricity plants powered by fuels such as coal and nuclear materials, around 2000 LMWh⁻¹ is consumed during operation whereas natural gas results in a substantially lower consumption of about 750 LMWh⁻¹.^[2] In the case of renewable energy sources, this energy-related water footprint (EWF) for solar thermal systems is high ($\approx 4000 \text{ LMWh}^{-1}$) whereas the EWF of biomass technologies is similar to that of coal. [2] Significantly lower EWF values are obtained for electricity provided by photovoltaics (PV) and wind energy (329 and 4 LMWh⁻¹, respectively),^[2] for which almost all of the water is consumed in the manufacturing stage.

On the flip side of the coin, one can examine the energy intensity for the provision of clean drinking water. Even

- [a] Prof. Dr. B. S. Richards Institute of Microstructure Technology (IMT) Karlsruhe Institute of Technology Hermann-von-Helmholtz-Platz 1 76344 Eggenstein-Leopoldshafen (Germany)
- [b] Prof. Dr. B. S. Richards Light Technology Institute (LTI) Karlsruhe Institute of Technology Engesserstrasse 13 76131 Karlsruhe (Germany)
- [c] J. Shen School of Engineering and Physical Sciences Heriot-Watt University Edinburgh, EH14 4AS (UK)
- [d] J. Shen, Prof. Dr. A. I. Schäfer Department of Water and Environmental Engineering Nelson Mandela African Institution of Science and Technology Arusha (Tanzania)
- [e] Prof. Dr. A. I. Schäfer Institute of Functional Interfaces (IFG) Karlsruhe Institute of Technology Hermann-von-Helmholtz-Platz 1 76344 Eggenstein-Leopoldshafen (Germany) E-mail: andrea.iris.schaefer@kit.edu
- IT This publication is part of a Special Issue on "Energy Research at Karlsruhe Institute of Technology".

To view the complete issue, visit: http://dx.doi.org/10.1002/ente.v5.7.

1.1944296, 2017, 7, Downloaded from https://onlinelbitary.wiley.com/doi/10.1002/ente.201600728 by Egyptian National St. Network (Enstinet) Wiley Online Library on [08/03/2023]. See the Terms and Conditions (https://onlinelbitary.wiley.com/terms-ad-conditions) on Wiley Online Library for rules of use; OA articles are governed by the applicable Creative Commons License

FULL PAPER



Figure 1. Examples of the water–energy nexus in today's society. Energy is needed for: 1) providing clean drinking water to our homes; pumping water from 6) lakes and rivers, and 7) underground; 8) powering desalination systems; 9) pressurizing water for irrigation systems; 13) driving advanced wastewater treatment systems; 14) collecting and treating wastewater; and 15) water heating and cooling systems. Conversely, water is required to: 2) operate hydropower plants; 3) operate cooling systems for all thermal power stations; 4) generate solar thermal energy; 5) mine and extract fossil energy resources; 10) irrigate biomass crops; 11) provide cooling at computer data centers; and 12) generate energy in anaerobic digestion plants (graphic adapted from Ref. [44]).

pumping freshwater from a groundwater source shallower than 60 m results in a specific energy consumption (SEC) of 0.14–0.24 kWhm⁻³ for pumping while large-scale conventional drinking-water treatment processes require about 0.36 kWhm⁻³, of which pumping of treated water makes the largest contribution.^[3] The energy required for classical four-stage water treatment—coagulation, sedimentation, filtration, and disinfection, followed by disinfection with chlorine and ammonia—amounts to about one-tenth of the total.^[4]

When more advanced water treatment, such as desalination processes, is required to remove dissolved salts from a water source, the energy intensity increases significantly. The SECs of thermally driven desalination processes are significantly higher than those of membrane-based technologies applied to large-scale seawater desalination, (7–14 and 2–6 kWhm⁻³, respectively).^[5]

While water scarcity can be addressed with energy-intensive solutions such as seawater desalination, other factors, such as climate change, population growth, and increased pollution, are also driving this trend toward energy-intensive treatment that increases the demand on less-potable water sources. However, in many geographic areas where water is both scarce and a limiting factor of health and economic development, no reliable electricity grid is available; this greatly restricts treatment options. At the global level, it has been reported that the world could face a 40% shortfall in water by 2030. [6]

Sub-Saharan Africa

There are few locations in the world that have such poor access to both clean drinking water and electricity as SSA. In 2015, the UN estimated that 663 million people in the world are still relying on unimproved drinking water sources, such as unprotected wells and springs and surface water, with over

half of the affected people living in SSA.^[7] In the same year, the International Energy Agency (IEA) determined 1.2 billion people in the world do not have access to electricity; again, more than half of the affected people (634 million) reside in SSA.^[8]

The situation is significantly worse in rural areas; herre, only 17% of rural SSA residents have access to electricity as opposed to 59% in the cities. Traditionally, this lack of largescale infrastructure has been viewed as a disadvantage, but more recent views consider that perhaps classical centralized water and electricity utilities are neither the most logical nor cost-effective solution in the remote regions of developing countries.^[9] This has been examined for provision of electricity in Africa by Szabó et al., who determined that photovoltaic power is the most viable option in several parts of Africa if consumers are able to pay €0.30 per kWh, which is cheaper than electricity provided by diesel generators, grid extensions, or other renewable sources.[10] Thus, there is a unique opportunity for integration of renewable energy in the water cycle exploiting productive synergies between water and energy systems.

The situation in Africa is explained graphically in Figure 2, which shows that all parts of Africa suffer from water scarcity or water stress.[11] Water scarcity refers to the physical abundance, or lack thereof, of a water supply whereas the concept of water stress is broader and includes water quality, the accessibility of water, and the recharge rate. In northern and southern Africa water scarcity is prevalent whereas throughout the remainder of the continent the lack of access to water is driven by economic factors. Reports in the literature indicate that water delivered by truck has a cost in the range of US\$2.40-9.67 per cubic meter of untreated drinking water. [12] Figure 2 b [13] shows that, except for Angola and Equatorial Guinea, typically 50-90% of the African population has access to an "improved" drinking water source. However, this largely refers to improved construction that prevents direct runoff and hence fecal contamination of the drinking water source and any other dissolved contaminants that may occur in the groundwater remain. An example of such contamination is shown in Figure 2c, in which fluoride concentrations exceeding the World Health Organization (WHO) guideline of 1.5 mg L⁻¹ occur.^[14]

Largely extending along the Rift Valley in eastern Africa, excessive fluoride in drinking water results in significant health problems, including dental and skeletal fluorosis. [15] More generally, a recent extensive study into the risk of groundwater contamination (see Figure 2d) indicates that a large belt of central and eastern Africa suffers from a moderate to very high risk, driven in part by the very shallow water table in these regions and ever-increasing agricultural activities. [16] In the same region, the inhabitants also have very poor access to electricity (see Figure 2e), often less than 25 %, and a few nations have a national electrification rate of 5 % or less. [17]

A lack of available energy in general is known to go handin-hand with human development and is inextricably linked with indicators such as life expectancy, illiteracy, and health.

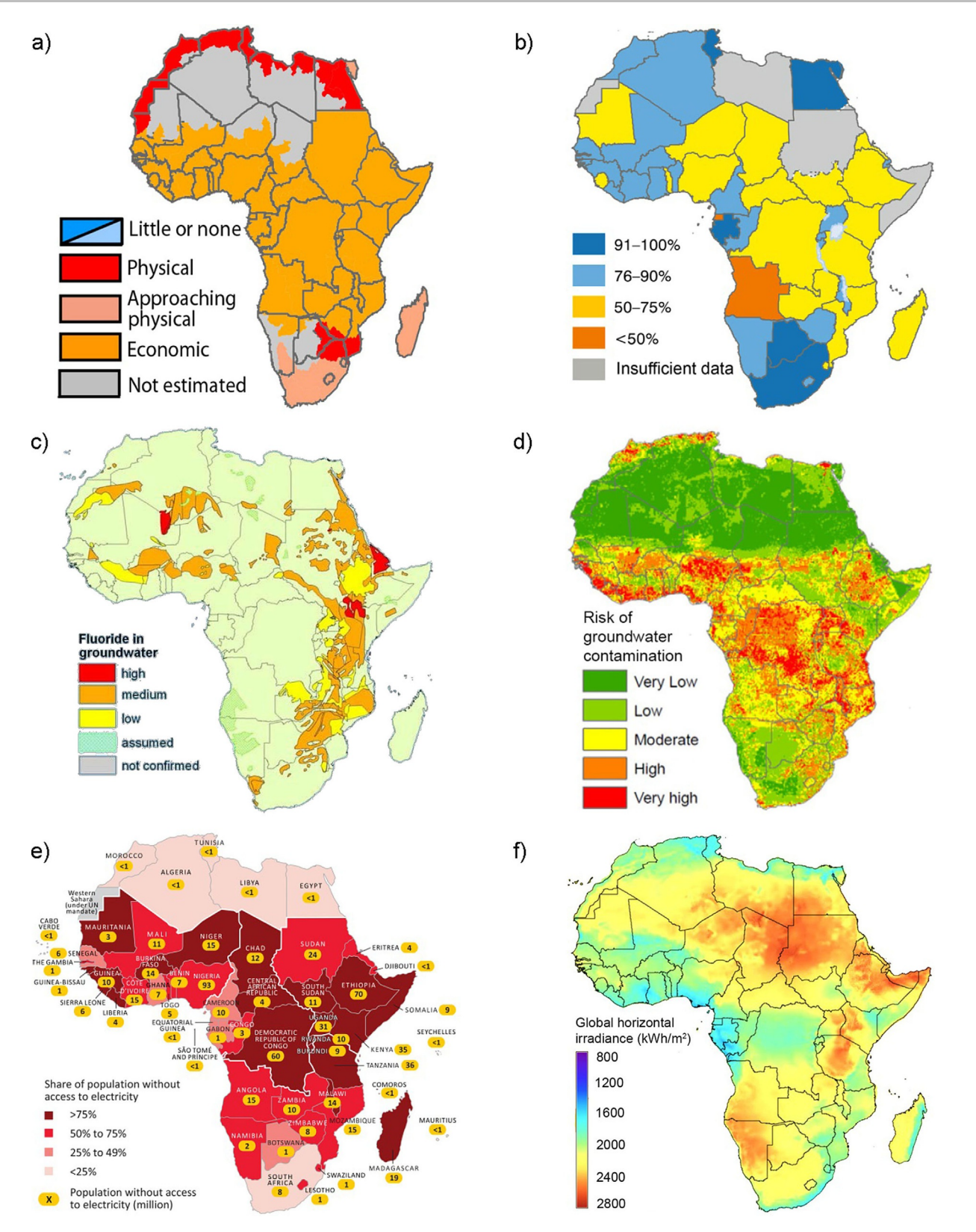


Figure 2. Six maps of Africa that illustrate the water–energy nexus: a) African areas suffering fresh-water stress and scarcity. [17] b) The fraction of the African population that has access to an "improved" water source. [7] c) An improved water source does not afford treatment; excess fluoride concentration in groundwater remains. [14] d) The overall risk of contamination of the groundwater in Africa was recently reported by Ouedraogo et al. [16] e) The fraction of the African population that does not have access to electricity. [17] f) The availability of solar irradiance across Africa. [19]

FULL PAPER

An example of the effect of "energy poverty" is shown in Figure 3, in which the countries that enjoy better access to electricity are the same as those more likely to fulfil the fundamental need for access to clean drinking water. At least 48% of the population of all African nations have access to improved drinking water sources whereas there is a large cluster of countries in which only 10–20% of the population have access to electricity. In contrast, the vast majority of developed countries have very close to 100% coverage for both electricity and clean drinking water.

Finally, to complete the picture, Figure 2 f indicates that the availability of global solar irradiance (incident on a horizontal surface) throughout all of Africa is truly excellent.^[19] Thus, the opportunity exists for solar energy technologies to break the energy-poverty cycle in Africa and, in this case, improve the access to clean drinking water.

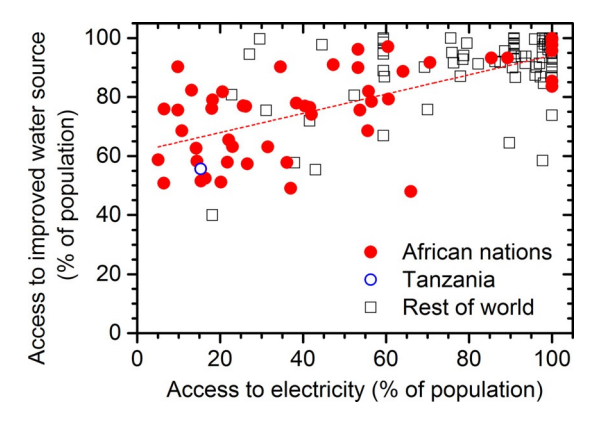


Figure 3. Correlation between the percentages of the population that have access to an improved drinking water source as a function of their access to electricity. Each data point represents one of 190 countries for which data was available, $^{[18]}$ with African countries plotted separately.

Theoretical energy consumption of water desalination

Desalinating seawater is relatively energy intensive. The thermodynamic limit indicating the amount of work theoretically needed to desalinate seawater can be derived as follows. A vessel is divided into two compartments, one of which contains seawater and the other freshwater, which are separated by a membrane that can only be permeated by water (system held at $25\,^{\circ}$ C). Due to a differential vapor pressure across the membrane, the natural forces of diffusion favor the freshwater being driven through the membrane to dilute the seawater. However, if an external pressure is applied to the compartment containing seawater, equilibrium can be reached, or even a flow in the reverse direction achieved. The pressure at equilibrium is known as osmotic pressure, and the amount of work W[J] required can be described as Equation (1): $^{[20]}$

$$W = \Pi dv \tag{1}$$

where dW is the amount of work required to achieve separation, Π the osmotic pressure [bar], and dv the volume [L] of

water permeating from the seawater side to the freshwater side.

From Equation (1), the first observation is that reducing the amount of work required for filtration is achieved by either reducing the pressure applied and/or the volume of water recovered. The required pressure can be reduced if the osmotic pressure of the solution is reduced. The value of Π is determined by using the van't Hoff equation, a reformulated version of the ideal gas law for liquids [Eq. (2)]:

$$\Pi = iMRT \tag{2}$$

where *i* is the experimentally determined van't Hoff constant, M the molarity of the solution [mol L⁻¹], R the gas constant $(8.314 \times 10^{-2} \text{ Lbar mol}^{-1} \text{ K}^{-1})$, and T the absolute temperature [K].

Assuming that seawater predominantly contains sodium chloride (NaCl, 58 gmol⁻¹) at a concentration of 35 gL⁻¹, then its molarity is 0.60 mol L^{-1} . The value for i in this case is 1.8 due to ion pairing. Hence, the osmotic pressure at 25 °C can be calculated by using Equation (2) to be $\Pi = 26.7$ bar. If the recovery of seawater is 0%—such that only an infinitesimally small amount of freshwater is recovered from a very large amount of seawater-then the minimum theoretical energy requirement is 2.6 kJ kg⁻¹ of fresh water produced, which equates to an SEC of 0.7 Wh L⁻¹ or, in the more typical units, 0.7 kWh m⁻³. As the recovery increases, so does the minimum SEC (0.8, 1.0, and 1.29 kWhm⁻³ at 25, 50, and 75%, respectively) due to increased electrical pumping requirements and real systems not operating as a reversible thermodynamic process.^[21] To this increase must be added the increase in concentration at the feed side due to salt rejection and concentration polarization, that is, higher concentration and hence osmotic pressure at the membrane surface. System design such as scale and component efficiencies further influence the real observed SEC.

Impact of water source and membrane characteristics on energy requirements

Brackish water represents a wide range of water sources that exhibit salinities in the range of 1–10 mg L⁻¹, that is, significantly lower than that of seawater. Equation (2) shows that for brackish water with a NaCl concentration of 3.5 gL⁻¹, ten times lower than that of seawater, the osmotic pressure is expected to decrease tenfold to Π =2.7 bar compared to seawater. Correspondingly, the experimentally determined SEC exhibits a strong dependence on salinity, with 3.8 and $1.5 \text{ kWh}\,\text{m}^{-3}$ for brackish water containing 10 and $1\,\text{gL}^{-1}$ NaCl, respectively.^[22] Note that, although it is not possible to optimize a single membrane system to efficiently treat such a wide salinity range, it does serve to demonstrate the strong dependence on the energy required to overcome the osmotic pressure of higher-salinity feed waters. This makes a very strong case for water reuse (treatment of secondary wastewater) over desalination, as the salinity in secondary effluent is typically about 1 gL⁻¹ whereas that of seawater is about 35 times higher. The same applies to surface or brackish waters,

FULL PAPER

which are much more favorable water sources than seawater if available.

A field-trip study indicated that the effect of treating the same borehole water using four different reverse osmosis (RO) membranes resulted in SECs varying from 2.3 to 1.3 kWhm⁻³.^[23] However, the permeate (clean water) produced by the membrane with the lowest SEC did not meet WHO drinking water guidelines for a specific contaminant (fluoride), highlighting the importance of selecting the correct membrane for a specific feed water and thus optimizing water quality and membrane permeability.

Membrane systems powered by renewable energy

Overall, significant progress has been made in reducing the SEC of RO desalination in the last four decades, and Elimelech and Phillip reported a factor-of-eight decrease in the case of seawater desalination. [21a] However, the lack of an electrical grid in remote locations extremely limits the penetration of membrane filtration systems. Building on the success of solar-driven water pumping systems, [24] photovoltaic-powered membrane filtration (PV-membrane) systems exhibit a number of key advantages: [5,25]

- Drinking water demand is typically highest when conditions are hot and sunny, which is exactly when the PVmembrane system produces more drinking water.
- 2) PV and RO are mature and robust technologies that require minimal maintenance.
- 3) PV and RO are based on modular technologies, enabling easy scaling of system sizes.

One weak point in PV-membrane system design is the inclusion of batteries; therefore, several research groups are pursuing batteryless systems^[26] and instead focus on robust system design and the storage of clean water. However, without an energy-storage system, the pump in the PV-membrane system is constantly presented with different current and voltage as solar radiation varies due to clouds, dust, and shade. PV-membrane system performance has been investigated under conditions of fluctuating and intermittent wind and solar energy under laboratory conditions. ^[26a,27] In addition, we have demonstrated that the use of supercapacitors can provide 2–4 min of energy buffering that results in an approximately 50% increase in the amount of clean drinking water produced over a 24-hour period. ^[27b]

A particularly relevant case for applications is the developing market, where little water and energy infrastructure exists and populations are sparse, and hence the opportunities for such sustainable and decentralized technologies exists. In the big picture, desalination needs to be considered as one possible solution for the provision of clean drinking water, along with rain-water harvesting and water reuse, for example; however, the ability to remove bacteria, viruses, and trace contaminants means that it can make many water sources fit for drinking that are currently inaccessible. The following case study describes such a scenario.

Case study: Water defluoridation in Tanzania

In a recent African study, the concept of water–energy nexus was extended to cover water, food, climate, and energy and its effect on sustainability and resilience investigated. Not surprisingly, it was found that security of supply for water, energy, and food are all inextricably linked and that a negative impact in one sector will often detrimentally affect both of the other sectors. Figure 3 shows that Tanzania is a relatively underdeveloped country that exhibits poor access to clean drinking water and electricity. A further security issue for food and water is that of flooding, with over 200000 people at risk from a 100-year flooding event in Dar es Salaam. [29] Further issues relating to water quality include contamination by heavy metals, sewage, and increased algal growth due to discharges from fertilizer factories. [30]

Further inland, there are two key issues. Firstly, there is a long dry season from June to October and a shorter one from January to February, meaning that for seven months of the year there is virtually no rainfall. Furthermore, the rainfall patterns have become more erratic and less reliable, with mean precipitation levels of about 500–750 mm a⁻¹.^[31] Secondly, the key problem in northern Tanzania is the natural occurrence of extremely high fluoride levels in both the surface and ground water of these volcanically active regions, [32] as shown in Figure 4. Whereas small amounts of fluoride



Figure 4. Saline soil deposits often coincide with high fluoride concentrations in surface water.

 $(<1~{\rm mg\,L^{-1}})$ are known to improve dental health, higher concentrations initially result in discoloration of the teeth (see Figure 5) and then, at higher concentrations $(>4~{\rm mg\,L^{-1}})$, in a debilitating bone disease called skeletal fluorosis. [15b] Tanzania is not alone with this problem, with an estimated 80 million people exhibiting the symptoms of fluorosis in East Africa, [33] but many of the residents simply have no alternative due to their economic circumstances.

While small-scale seawater desalination plants are currently being trialed in coastal regions, [34] the present work considers potential for applying RO systems to fluoride removal and for lower-pressure nanofiltration (NF) membranes, which require less power and thus have enhanced compatibility with PV. Szabó et al. predicted that PV can provide

electricity for less than €0.30 per kWh in many parts of Tanzania that are not reached by the grid, which is cheaper than other forms of electricity generation.[10]

In particular, this paper reports on the results of a field trip in which a PV-NF/RO system was tested in fluoride-contaminated waters in northern Tanzania and sought answers to the following questions: 1) What are the effects of different power availability on system performance? and 2) How does membrane choice affect water quality and energy requirements?

Research Methodology

PV-powered membrane filtration system

The PV-powered membrane filtration system, which incorporates an ultrafiltration (UF) membrane as a pretreatment stage for removal of viruses and bacteria, followed by an NF or RO membrane for salt and fluoride removal, is shown in Figure 6. The specifications of the system were originally published by Schäfer et al.^[35] (system) and Richards et al.^[27b] (sensors), while the modifications for the Tanzania field work were summarized by Shen et al. [32] The outputs from all sensors—current, voltage, electrical conductivity, flow, pressure, and temperature—are connected to a data logger (Datataker DT800), which is then connected to a PC running LabView. The system is designed to house one 4"-diameter, 40"-long NF/RO membrane module. Four different membrane modules were tested: BW30, BWLE, NF90 and NF270 (Dow Chemical, USA). Their characteristics, including aver-



Figure 6. Testing of the PV-powered NF/RO system at the NDRS.

age pore radii, are summarized in Table 1 and are classified as follows:

- 1) NF270: high-productivity NF membrane for removal of organics in medium-salinity water.
- 2) NF90: 90% salt removal, with high removal of iron, pesticides, herbicides, and organics.
- 3) BW30: high-rejection membrane for brackish water RO.
- 4) BW30-LE: low-energy version of BW30.

Case-study: Location and water quality

The chosen site for testing the PV-powered NF/RO system was the Ngurdoto Defluoridation Research Station (NDRS), located near the city of Arusha and between the dormant volcanoes Mt. Meru and Mt. Kilimanjaro, as shown in Figure 7. The drinking water available from the tap at the NDRS comes from a spring within Arusha National Park. The water quality analysis (see Table 2) indicates that, although the water is not very brackish, it contains a high fluoride concentration, which is 13 times greater than the WHO guideline limit of 1.5 mg L^{-1} .[36]

Water quality is essential to system performance and ultimately SEC. While the salinity of the water determines the osmotic pressure to be overcome, other factors such as likely foulants and scalants in the water add to the required energy. Tools to determine such potential fouling and scaling from water quality are speciation software (e.g., Visual MINTEQ[37]) and membrane-manufacturer software (e.g., ROSA by Dow Chemical^[38]). Speciation allows the pH- and

Table 1. Characteristics of NF/RO membranes investigated in this study with data provided by the manufacturer,[45] and the average pore radii.[46] n.a. = not available. All test conditions were at 15% recovery and 25°C; however, the salt type and operating pressure are different, which is normalized in the permeability values.

Membrane module	Active area [m²]	Permeate flux [Lh ⁻¹ m ⁻²]	Permeability [Lh ⁻¹ m ⁻²]	Average pore radius [nm]	Salt retention [%]	Manufacturer's test conditions
BW30	7.2	52.7	3.4	0.32	99.5	2 g L ⁻¹ NaCl at 15.5 bar
BW30-LE	7.2	55.0	5.3	n.a.	99.0	2 g L ⁻¹ NaCl at 10.3 bar
NF90	7.6	41.7	8.7	0.34	> 97.0	2 g L ⁻¹ MgSO ₄ at 4.8 bar
NF270	7.6	52.1	10.9	0.38-0.42	> 97.0	2 g L ⁻¹ MgSO ₄ at 4.8 bar

1.1944296, 2017, 7, Downloaded from https://onlinelbitary.wiley.com/doi/10.1002/ente.201600728 by Egyptian National St. Network (Enstinet) Wiley Online Library on [08/03/2023]. See the Terms and Conditions (https://onlinelbitary.wiley.com/terms-ad-conditions) on Wiley Online Library for rules of use; OA articles are governed by the applicable Creative Commons License

Figure 7. Location of the NDRS, near the city of Arusha in northern Tanzania (coordinates: S03°19.493′, E036°53.067′).

concentration-dependent calculation of species in the water. This allows potential changes in water quality and deposit formation when the pH of similar water sources changes to be understood. Figure 8 shows the MINTEQ-predicted speciation of four species that are likely to precipitate from this water: 1) fluoride, 2) carbonate, 3) calcium, and 4) magnesium. Fluoride shows one significant change in primary species at pH 3.2, which corresponds to its acid dissociation constant. Carbonate experiences two major changes, first from carbonic acid to bicarbonate at pH 6.4 and then from bicarbonate to carbonate at pH 10.2. Calcium exhibits one significant shift to its aqueous carbonate salt at pH 9.7. Similarly, mag-

Table 2. Water quality analysis of the NDRS tap water used in this study (ions analyzed as below detection limit are not reported).

Parameter	Unit	Value
pH (25 °C)	_	8.43
electrical conductivity (EC at 25 °C)	$\mu S cm^{-1}$	907
total dissolved solids (TDS) ^[a]	$mg L^{-1}$	637.6
turbidity	NTU	0.3
total organic carbon (TOC)	$mg L^{-1}$	1.3
inorganic carbon (IC)	mgL^{-1}	80.3
F ⁻	$mg L^{-1}$	20.2
Cl ⁻	mgL^{-1}	22.2
SO ₄ ²⁻	$mg L^{-1}$	32.2
Na ⁺	$mg L^{-1}$	184.4
K ⁺	mgL^{-1}	23.7
Ca^{2+} Mg^{2+} Sr^{2+}	$mg L^{-1}$	4.1
Mg ²⁺	$mg L^{-1}$	0.7
Sr ²⁺	$mg L^{-1}$	0.1

[a] Calculated as the sum of cations and anions; charge difference between cations and anions < 5%. The osmotic pressure of this water was calculated to be 0.5–0.6 bar.

nesium is converted to its carbonate at pH 10.5, but is then further converted to a hydroxide species above pH 11.

When the concentration at the membrane surface is enhanced, the species likely to precipitate can be identified. The saturation index (SI) indicates the likelihood of precipitation. SI>0 indicates likelihood for scale formation, and this likelihood increases with increasing temperature. In reality only waters with SI>0.5 exhibit significant scale formation. By more simple means, the SI can be determined by

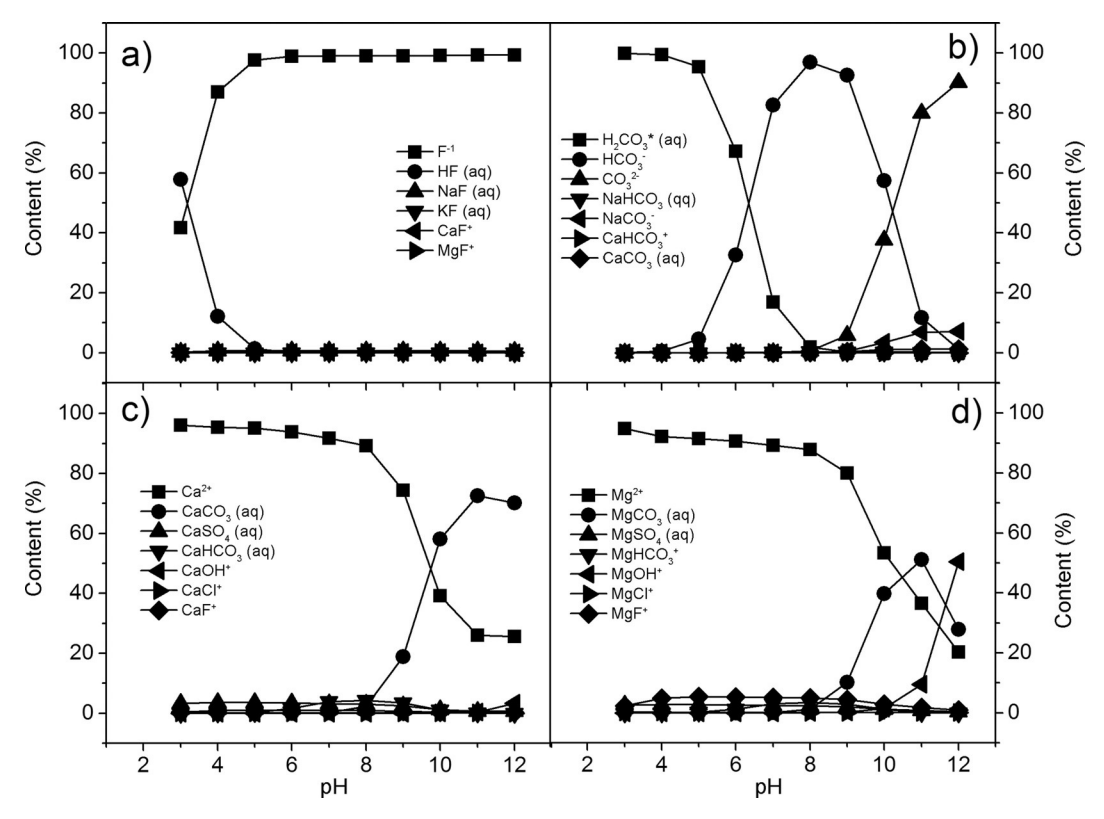


Figure 8. Water-quality speciation for the NDRS water determined by Visual MINTEQ 3.1: a) fluoride, b) carbonate, c) calcium, and d) magnesium species.

2194296, 2017, 7, Downloaded from https://onlinelbitary.wiley.com/doi/10.1002/ene.201000728 by Egyptian National Sti. Network (Enstine), Wiley Online Library on [08/03/2023]. See the Terms and Conditions (https://onlinelbitary.wiley.com/terms-and-conditions) on Wiley Online Library for rules of use; OA articles are governed by the applicable Creative Commons License

FULL PAPER

MINTEQ by assuming 100% retention or by ROSA by taking into account the typical retention of a particular module, operating conditions, and recovery. For the water studied in this work, the SIs of calcite (CaCO₃), fluorite (CaF₂), and dolomite (CaMg(CO₃)₂) as a function of recovery were predicted by MINTEQ 3.1 (Figure 9). In the case of

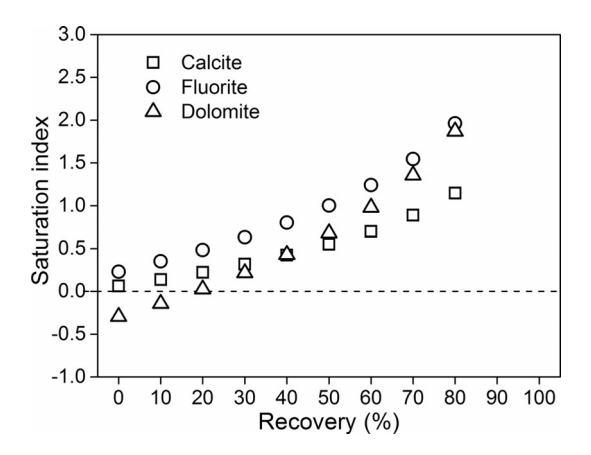


Figure 9. Saturation indices of several minerals as a function of recovery (assuming 100% retention) at 25 $^{\circ}$ C, obtained by using Visual MINTEQ 3.1.

this water, fluorite represents the only significant risk at recoveries below 50%. During the short-term experiments (maximum length typically a few hours) with the solar-powered membrane system reported in this paper, membrane fouling or scaling was not observed with this water. This will require longer-term operation and the investigation of the effect of fluctuation on fouling and scaling, which is unknown to date.

Results and Discussion

Impact of membrane choice on permeate water quantity, water quality, and SEC

Following the procedure described in the experimental section, a single set-point was identified with all membranes achieving a transmembrane pressure (TMP) of 5 bar and a feed flow of 510 Lh⁻¹ with an input power of 180 W. The PV-membrane system was then tested over a wide range of input powers and pressures ranging from 3 to 5 bar to map the system performance. Specifically, the main interest was the impact of membrane type, available power, and TMP on the SEC, provided safe drinking water could be produced.

Figure 10 shows the performance of the PV-membrane system in terms of feed flow, permeate flux, recovery, electrical conductivity (EC), and fluoride concentration of the permeate as well as the SEC. Figure 10a indicates that the feed flow rate to the BW30 membrane steadily increased as a function of power. In contrast, Figure 10b-d demonstrates that when the input power was greater than 240 W the feed flow for the BW30-LE, NF90, and NF270 membranes did not increase further, which is due to the pump reaching its

rotational speed limit (3000 rpm). The permeate flux (Figure 10e-h) did not exhibit a strong dependence on the power availability. However, flux increased on changing from a tighter (BW30) to a looser membrane (NF270) and at higher operating pressures. The recovery (ratio of permeate flow to feed flow, plotted in Figure 10i-l) decreased with increasing input power as a result of increasing feed flow and constant permeate flow.

The permeate fluoride concentrations of all four membranes decreased with increasing input power (Figure 10 mp). The transport of fluoride across the membrane involves both diffusion and convection.^[39] As mentioned above, input power determines the feed flow while TMP determines the permeate flux. On the one hand, an increase in feed flow increases turbulence and reduces the thickness of the concentration layer near the membrane surface. As a result, the diffusive transport contribution of fluoride decreases with increasing input power. On the other hand, the convective transport of fluoride is directly proportional to the permeate flux. At a fixed input power, higher permeate fluoride concentrations occurred at higher TMP, which is due to enhanced convective transport. The BW30 and BW30-LE membranes satisfy the WHO drinking-water guideline under all operating conditions while NF90 does so in most circumstances. In contrast, the NF270 membrane fails to meet the 1.5 g L^{-1} target.

The same mechanisms as described above likewise apply to the permeate EC (Figure $10\,\mathrm{q-t}$), and again the three tighter membranes give a permeate that is 10--20 times lower in salt concentration than that of the NF270 membrane. The permeate flow rate $[L\,h^{-1}]$ and power consumption [W] are needed to calculate the SEC $[Wh\,L^-$ or $kWh\,m^{-3}]$. Here, permeate flow rate is calculated from the permeate flux $[L\,m^{-2}\,h]$ multiplied by the membrane area. Figure $10\,u$ -x shows that the SEC increased as a function of input power, since the permeate production did not increase significantly with additional available power.

The experimental performance of the PV-membrane system (at the same set point) was compared to that expected from ROSA simulations (Figure 11). With increasing average pore radius (based on the retention of organic tracers) the permeate flux increases significantly (Figure 11a) such that the NF270 membrane exhibits three times higher flux than BW30. Figure 11 b shows that this increased flux incurs a lower SEC, which indeed drops below 0.5 kWh m⁻³ for NF270. However, Figure 11c demonstrates that this apparently good performance comes at a price: the water quality is much poorer. In particular, NF270 is the only membrane that produces water that is not able to meet the WHO limit for F-. This is a problem because the water will not taste salty or have any color or odor, and thus any normal consumer will not know that debilitating levels of F- remain in the treated water. The permeate fluoride concentration of the NF90 membrane at the set point is 1.38 mg L⁻¹, which is lower than the ROSA predicted value of 2.3 mg L⁻¹. However, in a previous study in which brackish water with higher fluoride concentration (47.6 mg L⁻¹) was treated, the perme-

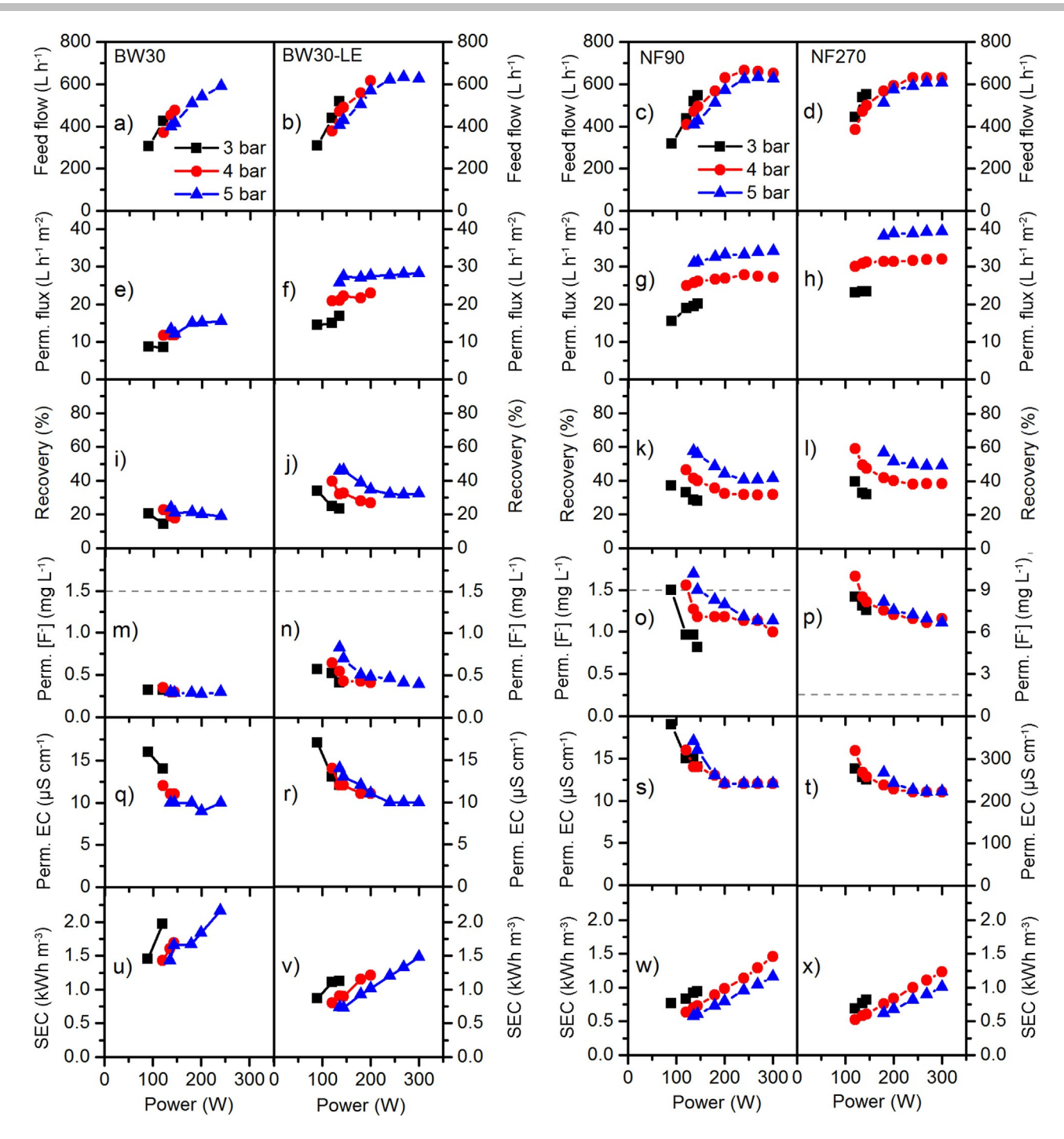


Figure 10. Performance of the PV-membrane system when equipped with four membranes (BW30-LE, BW30, NF90, and NF270) and at three set-point pressures (3, 4, and 5 bar) as a function of power in terms of feed flow (a-d), permeate flux (e-h), recovery (i-l), and permeate fluoride concentration (m-p), including the WHO guideline of 1.5 mg L⁻¹ for fluoride concentration in drinking water (dashed line), permeate electrical conductivity (q-t), and SEC (u-x). To facilitate comparison, graphs were plotted using the same y-axis scale; however, for p) and t) for the NF270 membrane, this was not possible.

ate fluoride concentration of NF90 under comparable operating conditions was even lower (0.9 $\rm mg\,L^{-1}).^{[40]}$ This implies complex effects of the raw water matrix on the retention of fluoride, which may involve various solute–solute and solute–membrane interactions. Further, both methods—ROSA and short-term experiments—do not take into account the long-term performance of the membrane. Membrane damage due to cleaning, fouling, scaling, and other factors will degrade retention performance with time. As a con-

sequence, even the NF90 membrane may not always meet the water-quality guidelines for this water.

The simulated recovery values (Figure 11 d) are consistently higher than the experimentally determined values. Generally, the simulation results lie within 15% of the experimentally determined values. The difference is attributed to: 1) the lack of a real pump model in the simulation software; 2) the complex nature of real water sources; and 3) the feedwater temperature in the simulation was fixed to 25°C, but

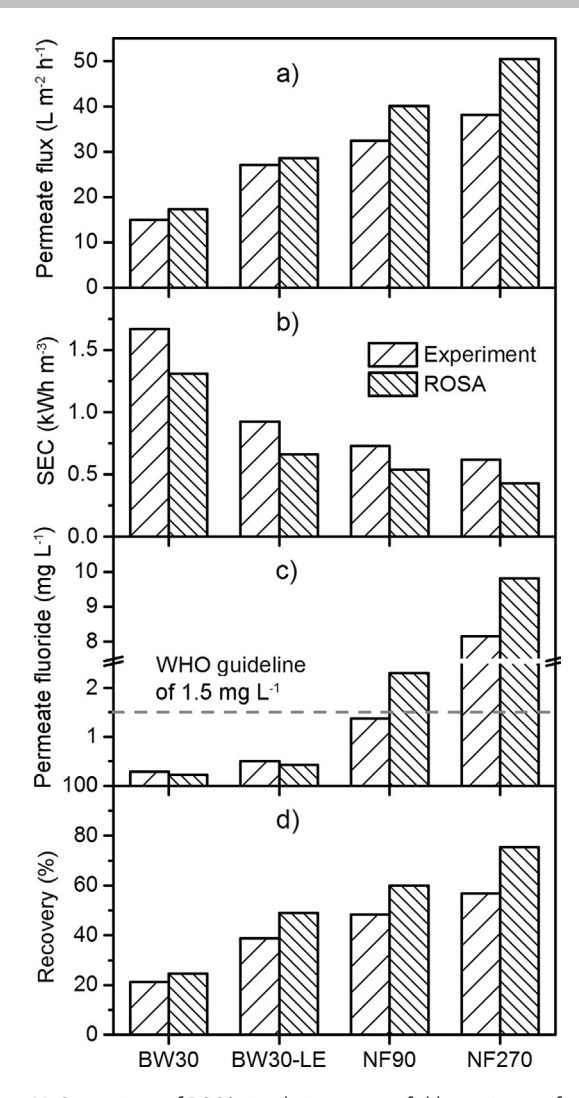


Figure 11. Comparison of ROSA simulations versus field experiments for the PV-membrane system equipped with four membranes (BW30, BW30-LE, NF90, and NF270) in terms of a) permeate flux, b) SEC, c) permeate fluoride concentration, including the WHO guideline of 1.5 mg L⁻¹ for fluoride concentration in drinking water (dashed line), and d) recovery.

in the field this value varied. Overall, the best results are obtained with the NF90 membrane, which offers high flux at a low SEC while still meeting the WHO guideline for F-concentration in drinking water during these experiments. The results confirm the retention data summarized by Shen and Schäfer.^[39] Although the results here indicate that the ROSA simulation tool can be used to select the best membrane for such a feed water and predict the system performance, for more complex waters containing, for example, natural organic matter this is a significantly more challenging task.

Outlook

The market potential for brackish-water desalination systems is potentially very large. As a starting point, the UN estimate of 663 million people who rely on unimproved drinking water sources can be taken.^[7] It can be assumed that the majority of the affected people 1) also do not have access to

electricity and 2) live in remote areas that require a decentralized solution. The WHO suggests that a minimum of 5 L of drinking water should be consumed per person each day, with an extra 20 L allowed for bathing. [36]

For the PV-membrane system described here a typical daily output is 2 m³ per solar day, which will cater for the drinking water needs of up to 400 people per day. Thus, a total of 1.7 million PV-membrane systems would be required to meet this demand. Clearly not all unimproved water sources require the removal of dissolved contaminants or desalination. However, the fraction of water sources that require this, or the enhancement of water availability that can be achieved by making nonpotable sources potable, is significant. The currently very high child mortality that results from poor water quality can be solved in many cases with ultrafiltration systems powered by renewable energy (or gravity). Such systems are of similar nature and significantly cheaper.

For the sake of estimating market potential, if a single PV-membrane system were to cost between US\$8000 and US\$100000^[9,41] an investment of US\$14-170 billion would be required to address this major problem by providing such decentralized units. In consequence, even a 1% share of this market would represent a business turnover greater than US\$140 million. Such an investment is unlikely to come from the governments of SSA nations directly; hence, attention must turn to the possible early adopters of such a technology, including international aid agencies, safari lodges, and eco-hotels. The above numbers explain the large number of companies that now engage in this technology, getting ready for a promising business to take off when donors have understood that such technologies may well be appropriate.

Note that SSA is not the easiest market-entry point for PV-powered water treatment technologies. Previous research has indicated that while securing financing remains a barrier, other sustainability issues make market penetration difficult, including the lack of skilled personnel for operation and maintenance, restricted or non-existent service networks, and limited availability of spare parts. [9] Furthermore, the socioeconomic integration and the adaptive capacity of communities also must be considered to ensure the development of technology that is appropriate to local needs and circumstances.

In terms of long-term economic sustainability, it can be assumed that the sale of the water from these systems will result in a self-financing business model that will allow for replacement of failed components over time. Indeed, water bottling factories maintain such systems in a very profitable manner and it can only be a matter of time until the less-exclusive fractions of the drinking-water market follow.

Most importantly, before a large number of decentralized and (largely) autonomous systems can be deployed in the remote regions of developing countries, long-term testing and a thorough evaluation of the robustness and reliability of the system are required. Such tests will lead to the correction of system component selection, full understanding of the long-term impact of operating a PV system with no energy

FULL PAPER

storage, the development of simple, yet effective, control systems, and the implementation of operation and maintenance strategies. Those pursuing such opportunities have a strong desire to see this technology emerge from the laboratory and make a difference in pursuing the goal: "I have a dream: safe water for all children!" [42]

Conclusions

Water and energy are intertwined in today's modern world. The extent of the water–energy nexus was reviewed, before highlighting the plight of the residents of one region of the world that has the poorest access to both clean drinking water and electricity worldwide, that is, sub-Saharan Africa (SSA). Many of these people live in remote areas and have not seen any benefits from the UN Millennium Development Goals. More novel "leapfrog" solutions are required to improve quality of life and health. The potential of decentralized photovoltaics (PV)-powered membrane filtration systems for the provision of potable water in areas that have no electricity grid and either contaminated or brackish water sources was highlighted.

In particular, the results of field work conducted in northern Tanzania were reported, where extremely high levels of fluoride naturally occur in the water sources and hence the removal of dissolved contaminants is required. Four different nanofiltration (NF) and reverse osmosis (RO) membranes were tested, three of which (BW30, BW30-LE, and NF90) were able to produce good-quality drinking water over a wide range of input powers. In particular, NF90 achieved the highest permeate production that still complied with World Health Organization (WHO) drinking-water guidelines while incurring the lowest specific energy consumption (SEC). Modeling using the ROSA software indicated good agreement with the experimental results (typically within 15%), thus indicating that carefully conducted water-quality analysis and simulations can be used to reliably predict the best choice of membrane to treat a water source with a relatively simple composition.

This project forms part of a long-term interdisciplinary research effort led by Richards and Schäfer that started in the early-2000s in outback Australia, [25a] was later adapted to run off wind power in Scotland, [27a,43] and then employed for extensive field-testing in Tanzania in 2013–2014. [32,39,40] By coupling fundamental research, application research, technology transfer, and industrial cooperation, the aim is to develop technology that can contribute to solving one of the biggest societal challenges: safe water without enhancing the energy crisis, taking advantage of the water–energy nexus.

Experimental Section

The performance of the PV-RO system equipped with different membranes for treating a particular feed water can only be compared under the same operating conditions. Therefore, an operational set point was determined for the NDRS water source by following the procedure described by Richards et al., [43] whereby

different membranes could be operated under the same TMP and feed-flow conditions. The two inputs that can alter TMP and feed flow are the input power and the setting of the regulating valve on the concentrate stream. A solar array simulator (SAS, Agilent Technologies E4350B-J02, USA) was used to power the 300 W DC pump of the system instead of PV panels to ensure reproducible solar-power quality for the experiments. With the same input power, membranes of different pore radius exhibit different TMPs. Thus, various combinations of input power and valve position were tested to identify a common set-point. The experimental procedure was as follows:

- 1) The SAS was set to simulate a PV array of 240 W,
- 2) The position of the regulating valve was carefully adjusted to achieve a desired TMP,
- 3) The resulting TMP and feed-flow values were recorded, and 4) The valve was readjusted to achieve a different TMP and flow rate and then step 2 was repeated.

At each operating point one permeate (filtered) sample was collected when steady-state conditions were reached, as indicated by constant conductivity and flow of both permeate and concentrate streams.

The membranes were tested in the sequence BW30, BW30-LE, NF90, and NF270. Before each test began, a cleaning procedure was conducted such that potential foulants and scalants that may have accumulated in the modules during experiments were removed. This involved: 1) a routine flush with RO water; 2) a routine cleaning schedule; 3) storing unused membranes in an antimicrobial solution, as wet and as cool as possible (not in direct sunlight); 4) repeating step 1 prior to fitting a new membrane in the system.

The experimental results were compared to that from the desalination software ROSA, [38] which is commonly used to design NF/RO water treatment systems that can meet the required drinking-water guidelines. For a given simulation, ROSA calculated the power required to pump the feed at a given pressure and flow rate and a pump efficiency of 43% was selected (the software is limited in terms of choosing pumps and operation). From this value, the SEC was then calculated by dividing by the permeate flow rate. The water temperature was assumed to be 25°C, and the flow factor was assumed to be 1, which is representative of a new membrane performing to specification. The BW30-LE module was not implemented in ROSA; therefore, a LC LE module was used as a replacement as suggested by the manufacturer.

Acknowledgements

A.I.S. and B.S.R. would like to acknowledge the financial support provided by Helmholtz Recruitment Initiative Fellowships, while a PhD scholarship for J.S. was provided by the Energy Technology Partnership (U.K.) together with the Drinking Water Quality Regulator for Scotland. Two Leverhulme Royal Society Africa Awards, SADWAT-Tanzania and SUCCESS, are acknowledged for partial project funding of the Tanzania field trip. The authors would like to express their gratitude to: Godfrey Mkongo (NDRS, Tanzania) for his hospitality, cooperation, and permission to carry out the experiments at NDRS, Geert Aschermann (TU Berlin, Germany) for assistance with conducting experiments in the field trial, Dow Chemical for generously donating many NF/RO mod-

FULL PAPER

ules, and GE Power & Water (Zenon) for the provision of the UF module.

Keywords: defluoridation • energy consumption membranes • nanofiltration • reverse osmosis

- [1] J. Macknick, R. Newmark, G. Heath, K. Hallett, *Environ. Res. Lett.* 2012, 7, 045802.
- [2] J. Fulton, H. Cooley, Environ. Sci. Technol. 2015, 49, 3314-3321.
- [3] F. Burton, Characteristics and Energy Management Opportunities, EPRI, Palo Alto, CA: September 1996. CR-106941, 1996.
- [4] R. Cohen, G. Wolff, B. Nelson, Energy Down the Drain: The Hidden Costs of California's Water Supply, NRDC/Pacific Institute, 2004, https://www.nrdc.org/sites/default/files/edrain.pdf.
- [5] A. Subramani, M. Badruzzaman, J. Oppenheimer, J. G. Jacangelo, Water Res. 2011, 45, 1907–1920.
- [6] L. Bizikova, D. Roy, D. Swanson, H. D. Venema, M. McCandless, The Water-Energy-Food Security Nexus: Towards a Practical Planning and Decision-Support Framework for Landscape Investment and Risk Management, IISD-International Institute for Sustainable Development, 2013, http://www.iisd.org/pdf/2013/wef_nexus_2013.pdf.
- [7] C. Way, The Millennium Development Goals Report 2015, UN, 2015, http://www.un.org/millenniumgoals/2015 MDG Report/pdf/ MDG%202015%20rev%20%28July%201%29.pdf.
- [8] A. Hoek, World Energy Outlook, International Energy Agency, 2015, http://www.worldenergyoutlook.org/weo2015/.
- [9] A. I. Schäfer, G. Hughes, B. S. Richards, Renewable Sustainable Energy Rev. 2014, 40, 542-556.
- [10] S. Szabó, K. Bódis, T. Huld, M. Moner-Girona, Environ. Res. Lett. 2011, 6, 034002.
- [11] D. Molden, Water for Food, Water for Life: A Comprehensive Assessment of Water Management in Agriculture, Earthscan, London, 2007, http://www.iwmi.cgiar.org/assessment/files_new/synthesis/Summary_ SynthesisBook.pdf.
- [12] a) H. M. A. Rossiter, P. A. Owusu, E. Awuah, A. M. MacDonald, A. I. Schäfer, Sci. Total Environ. 2010, 408, 2378–2386; b) S. Keener, M. Luengo, S. G. Banerjee, Provision of Water to the Poor in Africa: Experience with Water Standposts and the Informal Water Sector, AICD Working Paper 13, World Bank, Washington, DC, https:// dx.doi.org/10.1596/1813-9450-5387.
- [13] World Health Organization, and UNICEF. Progress on sanitation and drinking water—2015 update and MDG assessment, World Health Organization, 2015, http://files.unicef.org/publications/files/Progress_ on_Sanitation_and_Drinking_Water_2015_Update_.pdf.
- [14] R. Brunt, L. Vasak, J. Griffioen, Fluoride in Groundwater: Probability of Occurrence of Excessive Concentration on Global Scale, IGRAC-International Groundwater Resources Assessment Centre, Utrecht, 2004, https://www.un-igrac.org/resource/fluoride-groundwater-probability-occurrence-excessive-concentration-global-scale.
- [15] a) S. Ayoob, A. K. Gupta, Crit. Rev. Environ. Sci. Technol. 2006, 36, 433–487; b) J. K. Fawell, K. Bailey, Fluoride in drinking-water, World Health Organization, 2006, http://www.who.int/water_sanitation_health/publications/fluoride_drinking_water full.pdf.
- [16] I. Ouedraogo, P. Defourny, M. Vanclooster, Sci. Total Environ. 2016, 544, 939–953.
- [17] International Energy Agency (iea), Africa Energy Outlook: A Focus on Energy Prospects in Sub-Saharan Africa, IEA, Paris, 2014, https:// www.icafrica.org/en/knowledge-publications/article/africa-energy-outlook-a-focus-on-energy-prospects-in-sub-saharan-africa-263/.
- [18] World Bank, World Development Indicators, 2016, http://data.world-bank.org/products/wdi, accessed 21 October 2016.
- [19] T. Huld, R. Müller, A. Gambardella, Solar Energy 2012, 86, 1803– 1815.
- [20] M. Mulder, Basic Principles of Membrane Technology, Kluwer Academic, Dordrecht, 1996.
- [21] a) M. Elimelech, W. A. Phillip, Science 2011, 333, 712–717; b) V. G. Gude, Desal. Water Treat. 2011, 36, 239–260.

- [22] B. S. Richards, L. Masson, A. I. Schäfer, Appropriate Technologies for Environmental Protection in the Developing World (Ed.: E. K. Yanful), Springer, Dordrecht, 2009, pp. 123–137.
- [23] B. S. Richards, D. P. S. Capão, A. I. Schäfer, Environ. Sci. Technol. 2008, 42, 4563–4569.
- [24] a) P. S. Cartwright, Providing Safe Drinking Water in Small Systems: Technology, Operations, and Economics (Eds.: J. Cotruvo, G. F. Craun, N. Hearne), CRC Press, Boca Raton, FL, 1999, pp. 233–239; b) K. Meah, S. Fletcher, S. Ula, Renewable Sustainable Energy Rev. 2008. 12, 472–487.
- [25] a) B. S. Richards, A. I. Schäfer, Renewable Energy 2003, 28, 2013–2022; b) V. Fthenakis, A. A. Atia, O. Morin, R. Bkayrat, P. Sinha, Prog. Photovoltaics 2015, 24, 543–550.
- [26] a) B. S. Richards, D. P. Capão, W. G. Früh, A. I. Schäfer, Sep. Purif. Technol. 2015, 156, 379–390; b) A. M. Bilton, L. C. Kelley, S. Dubowsky, Desal. Water Treat. 2011, 31, 24–34; c) M. Thomson, D. Infield, Desalination 2005, 183, 105–111.
- [27] a) G. L. Park, A. I. Schäfer, B. S. Richards, J. Membr. Sci. 2011, 370, 34–44; b) B. S. Richards, G. L. Park, T. Pietzsch, A. I. Schäfer, J. Membr. Sci. 2014, 468, 224–232.
- [28] I. Chirisa, E. Bandauko, Urban Forum 2015, 26, 391-404.
- [29] A. S. Kebede, R. J. Nicholls, Reg. Environ. Change 2012, 12, 81-94.
- [30] S. M. Mohammed, Ambio 2002, 31, 617-620.
- [31] World Trade Press, *Precipitation Map of Tanzania*, **2007**, http://www.atozmapsdata.com/zoomify.asp?name=Country/Modern/Z_Tanzan_Precip, accessed 21 October 2016.
- [32] J. Shen, G. Mkongo, G. Abbt-Braun, S. L. Ceppi, B. S. Richards, A. I. Schäfer, Sep. Purif. Technol. 2015, 149, 349–361.
- [33] Endemic Fluorosis in Developing Countries: Causes, Effects and Possible Solutions (Ed.: J. E. Frencken), TNO Institute for Preventive Health Care, 1992, http://www.ircwash.org/resources/endemic-fluorosis-developing-countries-causes-effects-and-possible-solutions-report.
- [34] R. Yu, D. Packard, Cross-Cultural Commun. 2012, 8, 1, https://dx.doi.org/10.3968/j.ccc.1923670020120804.2001.
- [35] A. I. Schäfer, A. Broeckmann, B. S. Richards, *Environ. Sci. Technol.* 2007, 41, 998–1003.
- [36] World Health Organization, Guidelines for Drinking-Water Quality, 4th ed., WHO, 2011.
- [37] J. P. Gustafsson, Visual MINTEQ 3.0 User Guide, KTH, Sweden, 2011.
- [38] Dow Water & Process Solutions, ROSA System Design Software, 2016, http://www.dow.com/en-us/water-and-process-solutions/resources/design-software/rosa-software, accessed 29 September 2016.
- [39] J. Shen, A. I. Schäfer, Sci. Total Environ. 2015, 527-528, 520-529.
- [40] J. Shen, B. S. Richards, A. I. Schäfer, Sep. Purif. Technol. 2016, 170, 445-452.
- [41] U. Dehesa-Carrasco, J. Ramírez-Luna, C. Calderón-Mólgora, R. Villalobos-Hernández, J. Flores-Prieto, Water Sci. Technol. 2017, 17, 579–587.
- [42] D. Riecker-Schwörer, lookKIT, Vol. 3, Karlsruhe Institute of Technology, Karlsruhe, Germany, 2014, pp. 58–61, https://www.pkm.kit.edu/downloads/lookkit_2014_3.pdf.
- [43] B. S. Richards, G. L. Park, T. Pietzsch, A. I. Schäfer, J. Membr. Sci. 2014, 468, 400–409.
- [44] California Department of Water Resources, Water-Energy Nexus: Statewide, 2016, http://www.water.ca.gov/climatechange/WaterEnergyStatewide.cfm, accessed 14 Sept 2016.
- [45] Dow Filmtec, Water & Process Solutions Membrane Datasheets Filmtec BW30-4040, LC LE-4040, NF90-4040, NF270-4040, 2016, http://www.dow.com/en-us/water-and-process-solutions/products, accessed 21 October 2016.
- [46] a) A. J. Semião, A. I. Schäfer, J. Membr. Sci. 2013, 431, 244-256;
 b) L. A. Richards, B. S. Richards, B. Corry, A. I. Schäfer, Environ. Sci. Technol. 2013, 47, 1968-1976.

Manuscript received: November 23, 2016 Revised manuscript received: March 24, 2017 Accepted manuscript online: March 28, 2017 Version of record online: May 5, 2017